algorithms

MDPI

Article

Sine Cosine Algorithm Assisted FOPID Controller Design for Interval Systems Using Reduced-Order Modeling Ensuring Stability

Jagadish Kumar Bokam [1,*], Naresh Patnana [1], Tarun Varshney [2] and Vinay Pratap Singh [3,*]

[1] Electrical Engineering, National Institute of Technology Raipur, Chhattisgarh 492010, India; naresh283@gmail.com

[2] Electrical and Electronics Engineering, ABES Engineering College, Ghaziabad 201009, India; tarun.varshney@abes.ac.in

[3] Electrical Engineering, Malaviya National Institute of Technology Jaipur, Rajasthan 302017, India

* Correspondence: jagadishjaggu01@gmail.com (J.K.B.); vinay.ee@mnit.ac.in (V.P.S.); Tel.: +91-9989180291 (J.K.B.)

Received: 18 October 2020; Accepted: 23 November 2020 ; Published: 1 December 2020

Abstract: The focus of present research endeavor was to design a robust fractional-order proportional-integral-derivative (FOPID) controller with specified phase margin (PM) and gain cross over frequency (ω_{gc}) through the reduced-order model for continuous interval systems. Currently, this investigation is two-fold: In the first part, a modified Routh approximation technique along with the matching Markov parameters (MPs) and time moments (TMs) are utilized to derive a stable reduced-order continuous interval plant (ROCIP) for a stable high-order continuous interval plant (HOCIP). Whereas in the second part, the FOPID controller is designed for ROCIP by considering PM and ω_{gc} as the performance criteria. The FOPID controller parameters are tuned based on the frequency domain specifications using an advanced sine-cosine algorithm (SCA). SCA algorithm is used due to being simple in implementation and effective in performance. The proposed SCA-based FOPID controller is found to be robust and efficient. Thus, the designed FOPID controller is applied to HOCIP. The proposed controller design technique is elaborated by considering a single-input-single-output (SISO) test case. Validity and efficacy of the proposed technique is established based on the simulation results obtained. In addition, the designed FOPID controller retains the desired PM and ω_{gc} when implemented on HOCIP. Further, the results proved the eminence of the proposed technique by showing that the designed controller is working effectively for ROCIP and HOCIP.

Keywords: fractional calculus; fractional-order PID controllers; sine-cosine algorithm (SCA); continuous interval systems; modeling; Routh approximation

1. Introduction

In practical applications, many small modules are congregated to form a major dynamic system. The study, simulation and comprehensive analysis of such dynamic systems are carried out by means of mathematical modeling [1,2]. The derived mathematical models for such congregated systems, generally, turn out to be complex involving higher order transfer functions. The practical examples of higher order systems are as follows: nuclear reactors, power systems, chemical plants, etc. The controller design becomes a bit challenging for control engineers in these cases since the order of system is high [3]. In these cases, approximation of high-order transfer functions is advised to ease the controller design process [4,5]. The benefits of approximation include reduction in computational

complexity, simplified understanding of system and minimization in cost while designing hardware for the controller [6,7].

In industrial control applications, a proportional-integral-derivative (PID) controller is more popular. PID controller is used extensively due to its simple form and good performance. For tuning the gains of PID controllers, a large number of methods/algorithms have been developed in the literature. Over time, a significant development in fractional calculus is seen. Several studies have demonstrated the capabilities of fractional calculus in the field of pure mathematics [8,9], engineering [10,11], biological engineering [12] and physics [13]. It motivated the development of designing fractional order systems and controllers as far as control theory is concerned [14,15].

Many good articles are presented in the literature on the design of fractional-order PID (FOPID) controllers [16,17]. FOPID controller involves an additional pair of parameters (integral order and differential order) over an integer-order PID (IOPID) controller. These parameters provide better control if tuned properly. Similarly, these additional parameters are also seen as helpful in designing a system having robustness against high frequency noise signals, better disturbance rejection, etc. [18]. In [19], an FOPID controller is developed for fractional-order systems to achieve better performance over IOPID. An FOPID controller is designed for a five bar linkage robot based on modified PSO algorithm by Aghababa [20]. In [21], the robust stability analysis of fractional-order interval systems with multiple time delays and neutral systems is investigated.

Fractional integral-fractional derivative controller using small gain theorem and sensitivity function analysis to achieve desired PM and (ω_{gc}) is discussed by Azarmi et al. [22]. Liu and Zhang [23] designed an FOPID controller based on the Bode optimal reference model and flat phase property that ensures desired transient performance characteristics. This design is also robust to system parameter variations. Similarly, Saidi et al. [24] developed three new constrained numerical optimization algorithms for tuning the parameters of FOPID controller for delay-systems and parameter uncertain systems. In this case, it is seen that the property of iso-damping is enhanced. Bhookya et al. [25] proposed an FOPID controller based on the sine-cosine algorithm (SCA) optimization technique [26] for an automatic voltage regulator (AVR) system. Results showed that SCA tuned FOPID controller performance is superior in improving the transient response and is robust to external disturbance. An FOPID controller using SCA is designed to handle issues likes fluctuations in load and frequency, discontinuous power flow from wind turbines, etc. in a hybrid two-area power system by Khezri et al. [27].

Various strategies are available for model order reduction of higher order continuous and discrete interval systems. In [28], the low-order interval model is obtained using the stability equation technique, Kharitonov's theorem and minimization of integral-square-error (ISE) utilizing the differential evolution optimization technique. Singh et al. [29] adopted Routh–Pade approximation for order reduction of interval systems and also proposed two simple expressions for computing time moments (TMs) and Markov parameters (MPs). A thorough literature survey on model order reduction (MOR) methods based on Routh approximation for discrete and continuous interval systems is given in [30]. Later, the order reduction of higher order continuous interval systems is carried out using frequency domain reduction techniques [31] where the denominator of the model is derived from a differentiation method and the numerator is achieved using factor division, differentiation and Pade approximation methods. Another concept of order reduction of interval systems is stated depending on ISE minimization and impulse response energy using modified particle swarm optimization (PSO) algorithm by Anand et al. [32].

Model order reduction of linear time-invariant continuous and discrete interval systems based on Kharitonov's theorem using the differential method was presented by Potturu and Prasad [33]. The resulting interval model preserves all the dominant characteristics of original interval system. The frequency domain fractional-order controllers are designed generally based on the specifications [34] like phase margin, gain crossover frequency, steady-state error cancellation, high-frequency noise rejection and good output disturbance rejection. Authors in [35] extended the

differentiation method for reduced order modeling where the stability of lower order models is always guaranteed. In addition, it retains the initial TMs of higher order systems. Further, a new approach of order reduction based on the concept of impulse response gramian is developed in the frequency domain in [36]. Recently, Dewangan et al. [37] proposed a multipoint Routh–Pade approximation technique for single-input-single-output (SISO) and multi-input-multi-output (MIMO) interval systems. These methods assure a stable reduced model for higher order continuous interval systems.

This research presents a design of a robust fractional-order proportional-integral-derivative (FOPID) controller for reduced-order continuous interval plant (ROCIP) of higher-order continuous interval plant (HOCIP) based on considered frequency domain specifications using an advanced sine-cosine algorithm (SCA). Later, this controller is cascaded with HOCIP. Here, PM and ω_{gc} are considered as performance criteria of HOCIP for tuning the five parameters of FOPID controller. Since the design of the controller is done in the frequency domain, this approach guarantees the robustness and stability of the system. An improved Routh–Pade approximation method is utilized for reduced order modeling of HOCIP. The modified Routh table is utilized to derive the denominator polynomial of interval model whereas the coefficients of numerator polynomial are obtained by matching few TMs and MPs of system with those of the model. This order reduction technique always yields stable ROCIPs for stable HOCIPs. A third order interval plant is considered as an example to demonstrate the whole procedure of FOPID controller tuning and model order reduction. The efficiency of the proposed method for design of the FOPID controller is proved from the simulation results obtained.

The article is structured into seven sections: Section 1 includes the detailed literature survey on the present investigation. The preliminaries of fractional calculus and the structure of FOPID controller are given in Section 2. Problem formulation is briefed in Section 3. The design procedure for the proposed FOPID controller is illustrated in Section 4. In Section 5, the order reduction method for HOCIP is presented. Section 6 explains the SCA in detail. Section 7 includes the test case and its simulation results. Finally, the conclusions are reported in Section 8.

2. Preliminaries

2.1. Fractional Order Calculus

Recently, many systems are modeled as fractional-order systems utilizing fractional-order calculus. The fractional-calculus is found in several applications [34] in areas including electromagnetic waves [38], chemical engineering [39], signal processing [40], polymer science [41], electro-chemistry [42], neural networks [43], fluid mechanics [44], bio-engineering and bio sciences [45], control of power electronics [46], nonlinear control [47], etc.

The generalization of the integration and differentiation operators in fractional calculus [48] of k^{th} order is defined as

$$ {}_pD_q^k = \begin{cases} \frac{d^k}{dt^k} & \Re(k) > 0 \\ 1 & \Re(k) = 0 \\ \int_p^q (d\tau)^{-k} & \Re(k) < 0 \end{cases} \tag{1} $$

where p and q are the limits of the operation. The integration and differentiation of any real order can be performed. The Riemann–Liouville formula [49] for differentiation is given as

$$ {}_pD_q^k f(t) = \frac{1}{\Gamma(n-k)} \frac{\mathrm{d}^n}{\mathrm{d}t^n} \int_p^q \frac{f(\tau)}{(t-\tau)^{k-n+1}} \mathrm{d}\tau \tag{2} $$

where k can be any value in-between $(n-1)$ and n, and $\Gamma(.)$ is a Gamma function.

The Grünwald–Letnikov's definition of the fractional-order derivative [34] is expressed as

$$ {}_pD_q^k f(t) = \lim_{h\to 0} h^{-k} \sum_{a=0}^{\frac{(q-p)}{h}} (-1)^a \begin{pmatrix} k \\ a \end{pmatrix} f(t-ah) \tag{3} $$

where $(-1)^a \begin{pmatrix} k \\ a \end{pmatrix}$ are the binomial coefficients $C_a^{(k)}$, $(a = 0, 1, \ldots)$; and $[.]$ denotes the integer part. The formula given in [48] can be utilized to calculate the binomial coefficients.

The other commonly used formula for differentiation is known as Caputo expression [48]. The Caputo expression is defined as

$$ {}_pD_q^k f(t) = \frac{1}{\Gamma(n-k)} \int_p^q \frac{f^n(\tau)}{(t-\tau)^{k-n+1}} \, \mathrm{d}\tau \tag{4} $$

where $(n-1) < k < n$.

2.2. Fractional-Order PID (FOPID) Controller

The general formula for an FOPID controller [50] is depicted as

$$ \hat{C}(s) = K_a + \frac{K_b}{s^\alpha} + K_c s^\beta \tag{5} $$

which is commonly referred to as $PI^\alpha D^\beta$ controller where K_a, K_b, K_c are the proportional, integral and derivative gains, respectively. The parameters α and β indicate the positive real numbers [51]. In most of the engineering applications [23,50,52] the typical range of α and β variables lies with in $(0, 2)$ while designing FOPID controller. The primary benefits of the FOPID controller are achieved with extra tuning parameters namely α (non-integer order of integrator) and β (non-integer order of differentiation) as compared to conventional PID controller. As a result of these additional two parameters, FOPID controllers can be tuned in such a way that these may produce better control [53].

3. Problem Formulation

Suppose, an nth-order SISO continuous interval plant $G_n(s)$ for the closed-loop control system [54] of Figure 1 is expressed as

$$ G_n(s) = \frac{A(s)}{B(s)} = \frac{[A_0^-, A_0^+] + \cdots + [A_{n-1}^-, A_{n-1}^+]s^{n-1}}{[B_0^-, B_0^+] + [B_1^-, B_1^+]s + \cdots + [B_n^-, B_n^+]s^n} \tag{6} $$

The interval coefficients of numerator polynomial $A(s)$ are $[A_i^-, A_i^+]$ for $(i = 0, 1, \cdots, n-1)$, with A_i^+ as upper bounds and A_i^- as lower bounds, respectively. Likewise, interval coefficients of denominator polynomial $B(s)$ are $[B_i^-, B_i^+]$ for $(i = 0, 1, \cdots, n)$, with B_i^+ as upper bounds and B_i^- as lower bounds, respectively. The power series [55] form of HOCIP, (6), about $s = 0$ and $s = \infty$, respectively, are expressed as

$$ G_n(s) = \lambda_0 + \lambda_1 s + \cdots + \lambda_k s^k + \cdots \tag{7} $$

$$ G_n(s) = \mu_1 s^{-1} + \mu_2 s^{-2} + \cdots + \mu_k s^{-k} + \cdots \tag{8} $$

where $\lambda_i = [\lambda_i^-, \lambda_i^+]$ for $i = 0, 1, 2, \cdots$ and $\mu_i = [\mu_i^-, \mu_i^+]$ for $i = 1, 2, 3, \cdots$ are TMs and MPs of the interval system, respectively.

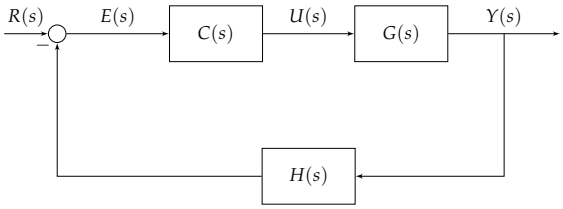

Figure 1. Block diagram of closed loop control system.

Figure 2 represents the closed-loop system without an FOPID controller. Figure 3 depicts the reduced-order model $\widehat{G_r}\ (s)$ of HOCIP in place of $G_n(s)$. The desired reduced-order continuous interval plant (ROCIP) $\widehat{G_r}\ (s)$ of $G_n(s)$ is represented as

$$\widehat{G_r}\ (s) = \frac{\widehat{E}\ (s)}{\widehat{F}\ (s)} = \frac{[e_0^-, e_0^+] + [e_1^-, e_1^+]s + \cdots + [e_{r-1}^-, e_{r-1}^+]s^{r-1}}{[f_0^-, f_0^+] + [f_1^-, f_1^+]s + \cdots + [f_r^-, f_r^+]s^r} \tag{9}$$

where $r < n$. The interval coefficients of numerator polynomial $\widehat{E}\ (s)$ are $[e_i^-, e_i^+]$ for $(i = 0, 1, \cdots, r-1)$, with e_i^+ as upper bounds and e_i^- as lower bounds, respectively. Similarly, the interval coefficients of denominator polynomials $\widehat{F}\ (s)$ are $[f_i^-, f_i^+]$ for $(i = 0, 1, \cdots, r)$ with f_i^+ as upper bounds and f_i^- as lower bounds, respectively. The model, (9), is expressed as

$$\widehat{G_r}\ (s) = \overset{\wedge}{\lambda}_0 + \overset{\wedge}{\lambda}_1 s + \cdots + \overset{\wedge}{\lambda}_k s^k + \cdots \quad \text{(expansion about } s = 0) \tag{10}$$

$$\widehat{G_r}\ (s) = \overset{\wedge}{\mu}_1 s^{-1} + \overset{\wedge}{\mu}_2 s^{-2} + \cdots + \overset{\wedge}{\mu}_k s^{-k} + \cdots \quad \text{(expansion about } s = \infty) \tag{11}$$

where $\overset{\wedge}{\lambda}_i = \left[\overset{\wedge}{\lambda}_i^-, \overset{\wedge}{\lambda}_i^+ \right]$ for $i = 0, 1, 2, \cdots$ and $\overset{\wedge}{\mu}_i = \left[\overset{\wedge}{\mu}_i^-, \overset{\wedge}{\mu}_i^+ \right]$ for $i = 1, 2, , 3, \cdots$ are TMs and MPs of ROCIP.

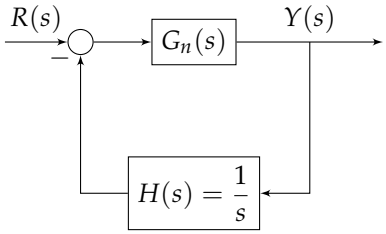

Figure 2. Closed loop system of HOCIP.

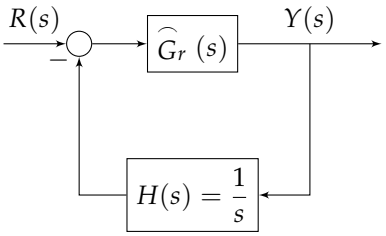

Figure 3. Closed loop system of ROCIP.

The model $\widehat{G_r}\ (s)$ in Figure 3 is an approximation of system $G_n(s)$ in Figure 2 which is obtained by order reduction technique. In this work, the denominator of $\widehat{G_r}\ (s)$ is obtained from improved Routh

approximation [56] and numerator of $\widehat{G_r}\ (s)$ is derived by matching of TMs and MPs [29]. Figure 4 shows the closed-loop control system with FOPID controller $\hat{C}\ (s)$ designed for ROCIP. Once the design for ROCIP is established, the same controller is applied to HOCIP as depicted in Figure 5 in order to ensure the applicability of designed controller for original system.

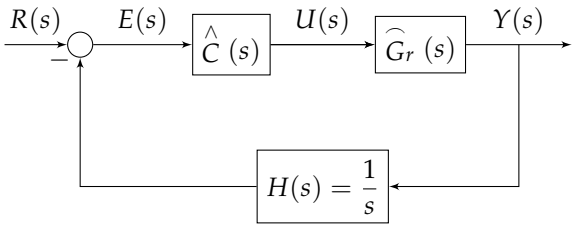

Figure 4. Closed loop ROCIP with FOPID controller.

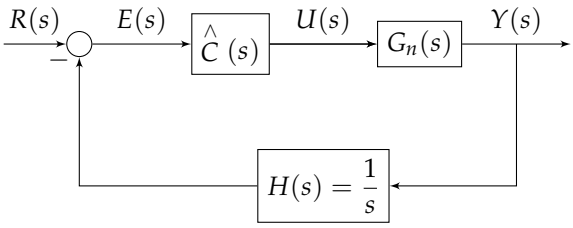

Figure 5. Closed loop HOCIP with FOPID controller.

4. Design of FOPID Controller

The procedure to design an FOPID controller ($PI^{\alpha}D^{\beta}$) for ROCIP to meet the desired performance is discussed in this section. The ROCIP of first order for (9) is given as

$$\widehat{G_1}\ (s) = \frac{[e_0^-, e_0^+]}{[f_0^-, f_0^+] + [f_1^-, f_1^+]s} \tag{12}$$

where e_0^- and e_0^+, respectively, are lower and upper limits of interval coefficient $[e_0^-, e_0^+]$ of the numerator of $\widehat{G_1}\ (s)$. Similarly, f_0^- and f_1^- are lower limits, and f_0^+ and f_1^+ are upper limits of interval coefficients $[f_0^-, f_0^+]$ and $[f_1^-, f_1^+]$.

The five unknown parameters of $PI^{\alpha}D^{\beta}$ controller are determined to satisfy the criteria of specified PM and ω_{gc}. These unknown design parameters of $PI^{\alpha}D^{\beta}$ controller are estimated by solving two non-linear equations [10,57,58]. The expressions given in (13) and (14) should be satisfied for a specified phase margin and gain crossover frequency [59].

$$20 * \log_{10} \left| \hat{C}\ (j\omega_{gc})\ \widehat{G}\ (j\omega_{gc}) H(j\omega_{gc}) \right| = 0 \tag{13}$$

$$Arg\Big(\hat{C}\ (j\omega_{gc})\ \widehat{G}\ (j\omega_{gc}) H(j\omega_{gc}) \Big) = -\pi + \phi_{pm} \tag{14}$$

4.1. Description of Fractional Order Controller Based on Bode Envelope

The transfer functions given in (15) and (16), respectively, offer the minimum and maximum plots of the gain.

$$\widehat{G_{1a}}\ (s) = \frac{e_0^-}{f_1^+ s + f_0^+} \tag{15}$$

$$\widehat{G_{1b}}\ (s) = \frac{e_0^+}{f_1^- s + f_0^-} \tag{16}$$

Similarly, the transfer functions given by (17) and (18), respectively, provide the minimum and maximum plots of the phase.

$$\widehat{G}_{1c}(s) = \frac{e_0^+}{f_1^- s + f_0^+} \tag{17}$$

$$\widehat{G}_{1d}(s) = \frac{e_0^-}{f_1^+ s + f_0^-} \tag{18}$$

Designing of $PI^{\alpha}D^{\beta}$ controller for $\widehat{G}_{1b}(s)$ and $\widehat{G}_{1d}(s)$ should satisfy (13) and (14), respectively. Thus, (13) and (14) become

$$20 * \log_{10} \left| \hat{C}(j\omega_{gc}) \widehat{G}_{1b}(j\omega_{gc}) H(j\omega_{gc}) \right| = 0 \tag{19}$$

$$Arg\left(\hat{C}(j\omega_{gc}) \widehat{G}_{1d}(j\omega_{gc}) H(j\omega_{gc}) \right) = -\pi + \phi_{pm} \tag{20}$$

Using the value of $\hat{C}(s)$ from (9), the expressions given in (19) and (20) become (21) and (22), respectively.

$$20 * \log_{10} \left| \left(\frac{e_0^+}{\sqrt{(f_1^- \omega_{gc})^2 + (f_0^-)^2}} \right) * \left(\sqrt{x^2 + y^2} \right) * \left(\frac{1}{\omega_{gc}} \right) \right| = 0 \tag{21}$$

$$tan^{-1}\left[\frac{y}{x}\right] - \frac{\pi}{2} - tan^{-1}\left(\frac{f_1^+ \omega_{gc}}{f_0^-} \right) = -\pi + \phi_{pm} \tag{22}$$

where

$x = K_a + K_b \omega_{gc}^{-\alpha} cos\left(\frac{\pi}{2}\alpha\right) + K_c \omega_{gc}^{\beta} cos\left(\frac{\pi}{2}\beta\right)$

$y = -K_b \omega_{gc}^{-\alpha} sin\left(\frac{\pi}{2}\alpha\right) + K_c \omega_{gc}^{\beta} sin\left(\frac{\pi}{2}\beta\right)$

The SCA is utilized for solving (21) and (22) to determine the unknown parameters of $\hat{C}(s)$.

5. Brief Description of Reduction Method for HOCIP

It is desired to approximate the system given in (6) into (9) based on improved Routh approximation integrated with matching of TMs and MPs. The former guarantees the stability and the latter improves overall response of reduced model.

5.1. Procedure for Denominator

The denominator polynomial $\widehat{F}(s)$ of ROCIP is obtained by using improved Routh table given in [56] which always ensures the stability of reduced model. The improved Routh table for denominator polynomial of HOCIP is given in Table 1.

Table 1. Modified Routh array.

$T_{1,1} = B_n$	$T_{1,2} = B_{n-2}$	$T_{1,3} = B_{n-4}$	$\cdots$
$T_{2,1} = B_{n-1}$	$T_{2,2} = B_{n-3}$	$\cdots$	
$T_{3,1}$	$T_{3,2}$		
$\vdots$	$\vdots$	$\ddots$	
$T_{n,1}$	$T_{n,2}$		
$T_{n+1,1}$			

The formula for calculating the interval elements of Table 1 is given as

$$T_{i,j} = T_{i-2,j+1} - \frac{\overset{\cap}{T}_{i-2,1}}{\overset{\cap}{T}_{i-1,1}} T_{i-1,j+1} \tag{23}$$

where $i \geq 3$ and $1 \leq j \leq (n-i+3)/2$. The element $\overset{\cap}{T}_{i,j}$ denotes the mid-point of the interval $[T^{-}_{i,j}, T^{+}_{i,j}]$ and its value is calculated according to

$$\overset{\cap}{T}_{i,j} = \frac{1}{2}\left(T^{-}_{i,j} + T^{+}_{i,j}\right) \tag{24}$$

While obtaining the elements of the modified Routh table (Table 1), two conditions are established to ensure the consistency of all elements.

Condition 1. *To ensure the existence of interval $T_{i,j}$, the element $T_{i-1,j+1}$ is modified to*

$$T_{i-1,j+1} = \left[\begin{array}{l} \max\left(T^{-}_{i-1,j+1}, \overset{\cap}{T}_{i-1,j+1} - \dfrac{UL_{i-2,j+1}}{2}\right), \\ \min\left(T^{+}_{i-1,j+1}, \overset{\cap}{T}_{i-1,j+1} + \dfrac{UL_{i-2,j+1}}{2}\right) \end{array}\right] \tag{25}$$

where $T^{-}_{i-1,j+1}$ and $T^{+}_{i-1,j+1}$ are the lower and upper bounds of the interval $T_{i-1,j+1}$; $\overset{\cap}{T}_{i-1,j+1}$ is the mid-point of interval $T_{i-1,j+1}$; $L_{i-2,j+1}$ is the range of element $T_{i-2,j+1}$ which is given as

$$L_{i-2,j+1} = T^{+}_{i-1,j+1} - T^{-}_{i-1,j+1} \tag{26}$$

and

$$U = \left(1/d\right)\left|\frac{\overset{\cap}{T}_{i-1,1}}{\overset{\cap}{T}_{i-2,1}}\right| \tag{27}$$

with $d > 1$. This value of d is obtained as

$$d = \frac{\left|\hat{T}_{i-1,1}\right| + \left|\overset{\cap}{T}_{i-2,1}\right|}{\left|\overset{\cap}{T}_{i-2,1}\right|} \tag{28}$$

Condition 2. *This condition sets essential features on the denominator polynomial obtained from the Table 1. The denominator polynomial, $\widehat{F}(s)$, of ROCIP is calculated from the $(n+1-r)$th and $(n+2-r)$th rows of Table 1 as*

$$\widehat{F}(s) = \overset{\cap}{T}_{n+1-r,1}\, s^{r} + T_{n+2-r,1} s^{r-1} + T_{n+1-r,2} s^{r-2} + \cdots \tag{29}$$

Usually, the value of $\overset{\cap}{T}_{n+1-r,1}$ is taken as the mid value of the interval $T_{n+1-r,1}$.

5.2. Procedure for Numerator

Once the denominator polynomial of ROCIP is obtained from (29), thereafter the interval coefficients of numerator polynomial are calculated by matching the first r interval TMs and MPs of HOCIP with ROCIP. This can be expressed mathematically as:

$$\left[\lambda_i^{-}, \lambda_i^{+}\right] = \left[\begin{array}{c} \overset{\wedge}{\lambda}_i^{-}, \overset{\wedge}{\lambda}_i^{+} \end{array}\right] \quad \text{for} \quad i = 0, 1, \cdots, (\psi - 1) \tag{30}$$

$$[\mu_i^-, \mu_i^+] = \left[\overset{\wedge}{\mu}_i^{-}, \overset{\wedge}{\mu}_i^{+} \right] \quad \text{for} \quad i = 1, 2, \cdots, \sigma \tag{31}$$

where $\psi + \sigma = r$. To achieve a better steady-state response of ROCIP, at least one TM should be considered [60] such that $\psi \geq 1$. The general expression for calculating interval TMs and interval MPs for continuous interval system are proposed by Singh et al. [29]. The expressions for $[\lambda_m^-, \lambda_m^+]$ and $[\mu_m^-, \mu_m^+]$ parameters for HOCIP, (6), are given as:

$$[\lambda_m^-, \lambda_m^+] = \frac{[A_m^-, A_m^+]}{[B_0^-, B_0^+]} - \sum_{i=0}^{m-1} \frac{[B_{k-i}^-, B_{k-i}^+][\lambda_i^-, \lambda_i^+]}{[B_0^-, B_0^+]} \qquad m = 0, 1, 2, \cdots \tag{32}$$

$$[\mu_m^-, \mu_m^+] = \frac{[A_{n-m}^-, A_{n-m}^+]}{[B_n^-, B_n^+]} - \sum_{i=1}^{m-1} \frac{[B_{n-k+i}^-, B_{n-k+i}^+][\mu_i^-, \mu_i^+]}{[B_n^-, B_n^+]} \qquad m = 1, 2, \cdots \tag{33}$$

In the same manner, the expressions for ROCIP, (9), are written as

$$\left[\overset{\wedge}{\lambda}_m^{-}, \overset{\wedge}{\lambda}_m^{+} \right] = \frac{[e_m^-, e_m^+]}{[f_0^-, f_0^+]} - \sum_{i=0}^{m-1} \frac{[f_{k-i}^-, f_{k-i}^+] \left[\overset{\wedge}{\lambda}_i^{-}, \overset{\wedge}{\lambda}_i^{+} \right]}{[f_0^-, f_0^+]} \qquad m = 0, 1, 2, \cdots \tag{34}$$

$$\left[\overset{\wedge}{\mu}_m^{-}, \overset{\wedge}{\mu}_m^{+} \right] = \frac{[e_{r-m}^-, e_{r-m}^+]}{[f_n^-, f_n^+]} - \sum_{i=1}^{m-1} \frac{[f_{r-k+i}^-, f_{r-k+i}^+] \left[\overset{\wedge}{\mu}_i^{-}, \overset{\wedge}{\mu}_i^{+} \right]}{[f_r^-, f_r^+]} \qquad m = 1, 2, \cdots \tag{35}$$

6. Sine-Cosine Algorithm (SCA)

The SCA initially creates a set of random population and allows them to move towards the best solution. In this algorithm, the optimization process contains two phases namely exploration and exploitation which lead to produce global (best) solution. The trigonometric functions namely sine sine and cosine functions are used to update the solutions in this algorithm. The position is updated as:

$$V_p^{k+1} = V_p^k + \beta_1 * sin(\beta_2) * |\beta_3 Q_p^k - V_p^k| \qquad \beta_4 \geq 0.5 \tag{36}$$

$$V_p^{k+1} = V_p^k + \beta_1 * cos(\beta_2) * |\beta_3 Q_p^k - V_p^k| \qquad \beta_4 < 0.5 \tag{37}$$

where V_p^{k+1} and V_p^k are old and updated positions of current solution at k-th iteration in p-th dimension. Q_p^k is the position of destination point in k-th dimension. The parameters β_2, β_3 and β_4 are random numbers in the range of $[0, 1]$. However, $|.|$ represents the absolute value.

The distinctive features of sine and cosine functions of (36) and (37) are shown in Figure 6. By varying the value of β_1, the amplitude of sine and cosine functions can be altered which results in finding a solution outside the space between their corresponding boundaries. Figure 7 shows exploration and exploitation of search space with sine and cosine wave-forms lying between $[-2, 2]$. In SCA algorithm, the balance exploration and exploitation can be achieved by changing β_1 using

$$\beta_1 = a - k\frac{a}{T} \tag{38}$$

where k is the current iteration, T is the total number of iterations and a is constant.

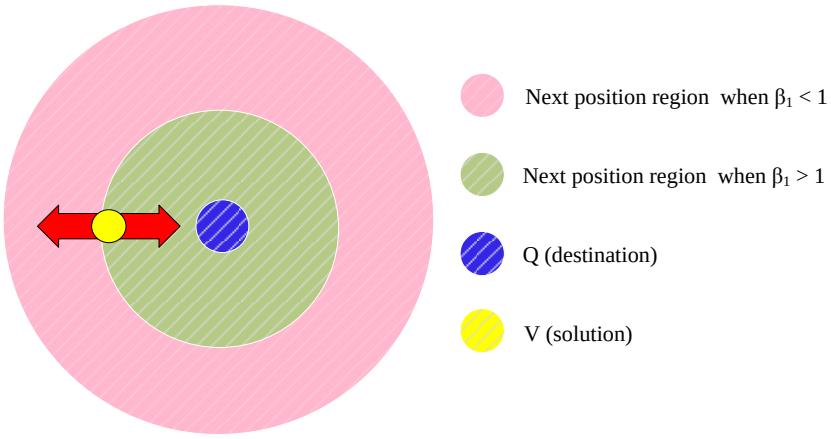

Figure 6. The result of the sine and cosine functions in (36) and (37) for the next stage [26].

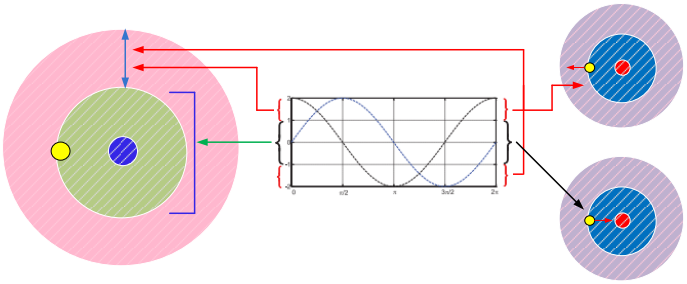

Figure 7. Sine and cosine functions within the range of $[-2, 2]$ allow a way to move around (inside the space among them) or beyond (outside the space among them) the target [26].

7. Test System

This section consists of two parts. In the first part, a test case is taken to explain model order reduction technique. In the second part, the design procedure of the FOPID controller for ROCIP is elaborated.

7.1. Improved Routh–Pade Approximation Method

Let the third-order SISO test system be given as

$$G_3(s) = \frac{[3,4]s^2 + [25,26]s + [14,15]}{[7,8]s^3 + [54,55]s^2 + [90,91]s + [35,36]} = \frac{A(s)}{B(s)} \tag{39}$$

The desired first-order model for (39) becomes

$$\widehat{G_1}\ (s) = \frac{[e_0^-, e_0^+]}{[f_0^-, f_0^+] + [f_1^-, f_1^+]s} = \frac{\widehat{E}\ (s)}{\widehat{F}\ (s)} \tag{40}$$

7.1.1. Calculation of Denominator

The improved Routh Table (Table 1) for denominator of (39) obtained using (23) is given in Table 2.

Table 2. Routh array for denominator polynomial of (39).

s^3	$[7,8]$	$[90,91]$
s^2	$[54,55]$	$[35.06, 35.94]$
s^1	$[85.175, 86.054]$	
s^0	$[35.06, 35.94]$	

The denominator of (40) is obtained from direct truncation of Table 2 which is given as

$$\widehat{F}\ (s) = [85.175, 86.054]\, s + [35.06, 35.94] \tag{41}$$

7.1.2. Calculation of Numerator

The first interval TM and first interval MP of HOCIP, (39), are determined using (32) and (33), which are given as

$$[\lambda_0^-, \lambda_0^+] = [0.389, 0.428] \tag{42}$$

$$[\mu_1^-, \mu_1^+] = [0.375, 0.571] \tag{43}$$

The numerator polynomial of the desired first-order model, (40), can be obtained by matching first interval TM of HOCIP with first interval TM of ROCIP, such that

$$[\overset{\wedge}{\lambda}_0^-, \overset{\wedge}{\lambda}_0^+] = [\lambda_0^-, \lambda_0^+] \tag{44}$$

Using (34) and (42), the numerator polynomial is obtained as

$$\widehat{E}\ (s) = [e_0^-, e_0^+] = [13.638, 15.382] \tag{45}$$

Therefore, the desired first-order interval model, $\widehat{G_1}\ (s)$, obtained from (41) and (45), is given as

$$\widehat{G_1}\ (s) = \frac{[13.638, 15.382]}{[85.175, 86.054]s + [35.06, 35.94]} \tag{46}$$

Figure 8 represents the step response of interval transfer function (39) and its proposed model (46). It is clear from Figure 8 that the steady-state response of proposed model (46) and the system (39) are exactly identical, but when it comes to the transient state response there is a slight deviation between (39) and (46). Therefore, it can be concluded safely that the model preserves essential characteristics of the original system. This illustrates that proposed model (46) provides a good model of system (39).

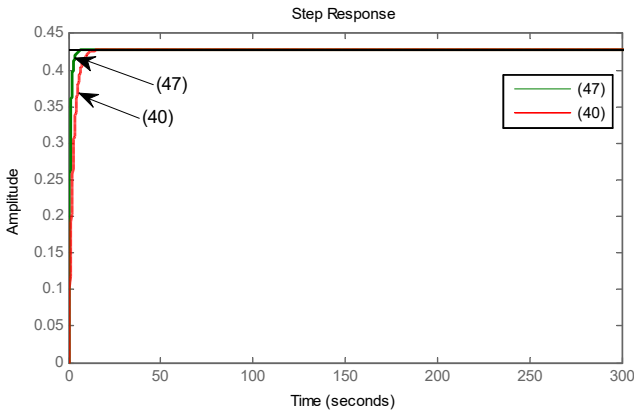

Figure 8. Step response of system $G_3(s)$ and model $\widehat{G_1}\ (s)$.

7.2. Design of FOPID Controller

An SCA-based FOPID controller is proposed for the first order interval system, (46), by considering the frequency domain specifications. In order to establish the efficacy of the SCA-based FOPID controller, other algorithms, namely particle swarm optimization (PSO) [61], Nelder–Mead simplex (NMS) [4] and Luus–Jaakola (LJ) [62,63] are also used to obtain the parameters of $PI^{\alpha}D^{\beta}$ controller. A total of 50 candidates are considered in whole population with 100 iterations for all algorithms.

The key feature of the SCA algorithm [61,64–66] is that it is free from algorithm-specific parameters. The algorithm-specific parameters of all other algorithms are listed in Table 3.

Table 3. Algorithm-specific parameters for different algorithms.

Algorithms	Parameters	Values
PSO	Cognitive parameter, c_1	2
	Social parameter, c_2	2
	Inertia weight, w	0.5
NMS	Refection coefficient, α	1
	Contraction coefficient, β	1/2
	Expansion coefficient, γ	2
	Shrinking coefficient, δ	1/2
LJ	Contraction factor, γ	0.95
SCA	No parameter	–

In order to design the FOPID controller, different transfer functions are constructed as shown in Section 4.1. Using (16) and (18), the system transfer functions corresponding to maximum plots of gain and phase of the Bode envelope given as

$$\widehat{G}_{1b}(s) = \frac{15.382}{85.175s + 35.06} \tag{47}$$

$$\widehat{G}_{1d}(s) = \frac{13.638}{86.054s + 35.06} \tag{48}$$

The design criteria of the controlled system are considered as: gain crossover frequency (ω_{gc})= 50 rad/sec and phase margin (ϕ_{pm})= 85 deg.

Figure 9 represents the block diagram of ROCIP with an SCA-based FOPID controller. To obtain the desired specifications, (21) and (22) are solved using SCA. The optimal parameters (K_a, K_b, K_c, α and β) of $PI^{\alpha}D^{\beta}$ controller obtained are

$$K_a = 324.565, K_b = 658.081, K_c = 204.214, \\ \alpha = 0.616, \beta = 0.992 \tag{49}$$

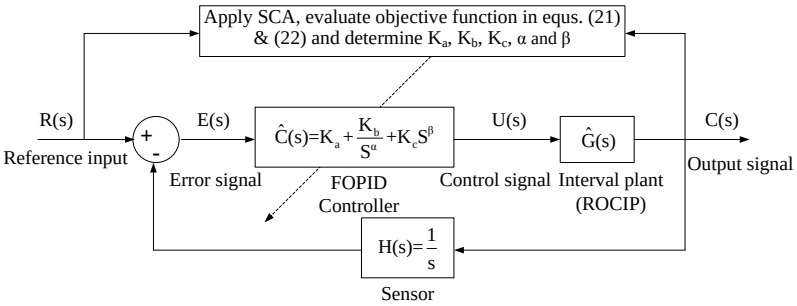

Figure 9. ROCIP with an SCA-based FOPID controller.

The FOPID controller for the specified design criteria is given as

$$\hat{C}(s) = 324.565 + \frac{658.081}{s^{0.616}} + 204.214s^{0.992} \tag{50}$$

The FOPID controllers for the above defined specifications obtained due to PSO, NMS and LJ are given as

$$\hat{C}_{PSO}(s) = 245.496 + \frac{335.474}{s^{0.457}} + 443.675s^{0.845} \tag{51}$$

$$\hat{C}_{NMS}(s) = 832.765 + \frac{147.164}{s^{0.329}} + 379.852s^{0.693} \tag{52}$$

$$\hat{C}_{LJ}(s) = 473.359 + \frac{259.876}{s^{0.478}} + 156.952s^{0.573} \tag{53}$$

Figure 10 presents the unit step response of closed-loop control system of Figures 4 and 5 having ROCIP and HOCIP, respectively. From Figure 10, it is clearly observed that the designed FOPID controller $\hat{C}(s)$ using SCA for ROCIP, $\widehat{G_1}(s)$, is also suited for HOCIP, $G_3(s)$. This establishes the usefulness of proposed technique.

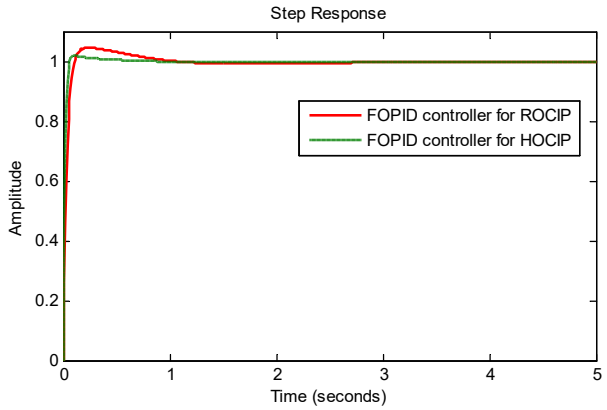

Figure 10. Unit step response of controlled ROCIP and HOCIP.

Figure 11 depicts the Bode plots of the open-loop controlled systems with FOPID controller. It is clear from the Figure 11 that frequency response of the SCA-based FOPID controller is also excellent for both ROCIP and HOCIP.

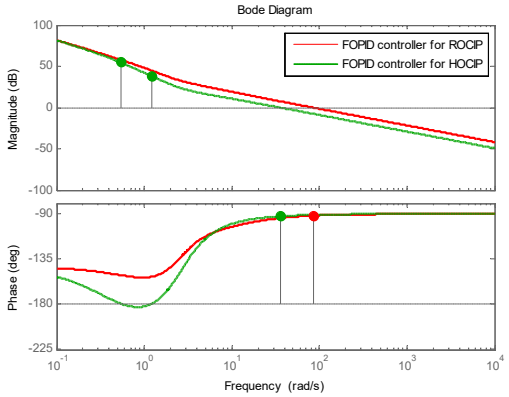

Figure 11. Bode plots of controlled ROCIP and HOCIP with an FOPID controller.

Figures 12 and 13 plots the step responses of ROCIP and HOCIP with FOPID controllers obtained due to SCA, PSO, NMS and LJ. However, Figures 14 and 15 are showing the Bode plots. It is clearly observed that the step responses of the closed-loop system with an SCA-based FOPID controller is better when compared to other optimization algorithms. The same is true for frequency response plotted in Figures 14 and 15. This clearly established the supremacy of the SCA-based FOPID controller.

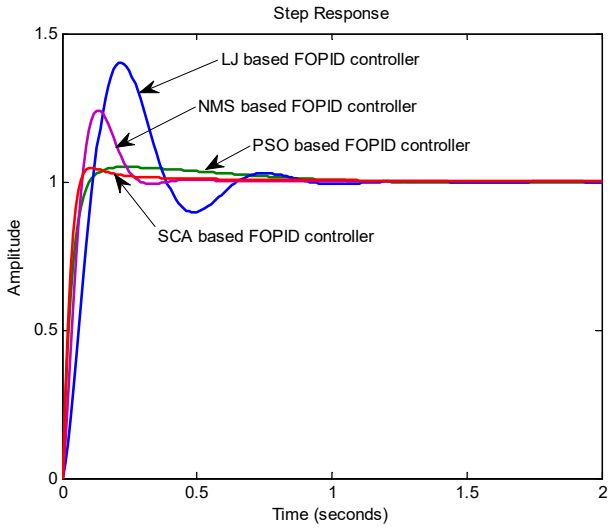

Figure 12. Step response of controlled ROCIP with the FOPID controller.

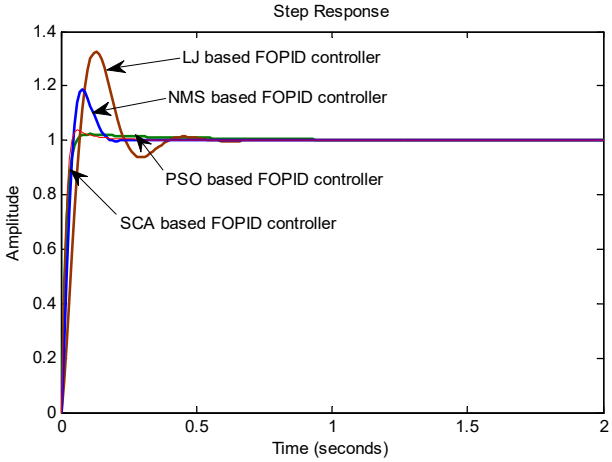

Figure 13. Step response of controlled HOCIP with the FOPID controller.

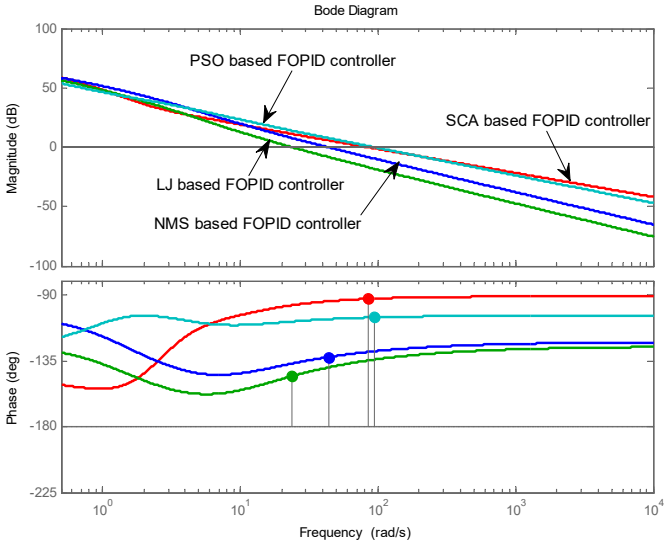

Figure 14. Bode response of controlled ROCIP with FOPID controller

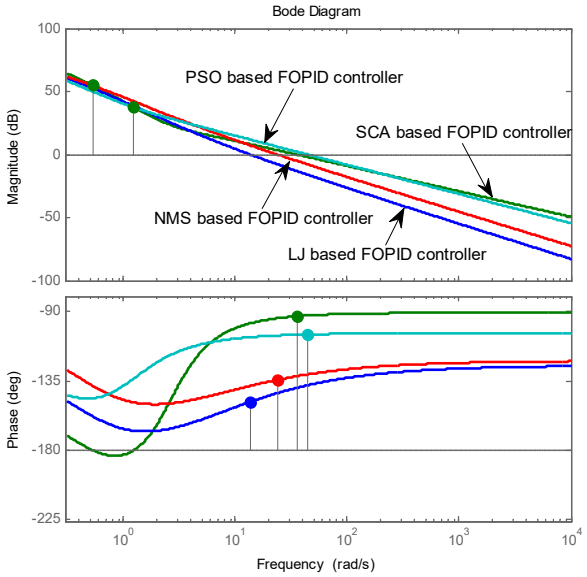

Figure 15. Bode response of controlled HOCIP with the FOPID controller.

The comparative analysis is reported in Table 4. It is seen that the desired frequency domain specifications (ω_{gc}= 50 rad/sec and ϕ_{pm}= 85 deg) of HOCIP are nearly fulfilled with an SCA assisted FOPID controller. The FOPID controllers designed using SCA, PSO, NMS, and LJ optimization techniques for HOCIP gives frequency domain specifications as (ω_{gc}= 87.32 rad/sec and ϕ_{pm}= 54.7 deg), (ω_{gc}= 75.83 rad/sec and ϕ_{pm}= 43.2 deg), (ω_{gc}= 58.57 rad/sec and ϕ_{pm}= 28.3 deg) and (ω_{gc}= 31.54 rad/sec and ϕ_{pm}= 33.7 deg), respectively. From these values, it is evident that the ω_{gc} and ϕ_{pm} obtained from the FOPID controllers designed using PSO, NMS and LJ are having larger deviations from the desired frequency domain specifications when compared to the FOPID controller based on SCA. This proves that the designed controller $\hat{C}(s)$ is robust and also best suited for both ROCIP and HOCIP to attain the desired specifications.

Table 4. Controller parameters and specifications for different algorithms.

Algorithms	ϕ_{pc} (deg)	ω_{gc} (rad/sec)	K_a	K_b	K_c	α	β
SCA	87.32	54.7	324.565	658.081	204.214	0.616	0.992
PSO	75.83	43.2	245.496	335.474	443.675	0.457	0.845
NMS	58.57	28.3	832.765	147.164	379.852	0.329	0.693
LJ	31.54	33.7	473.359	259.876	156.952	478	0.573

8. Conclusions

This article proposed a robust $PI^{\alpha}D^{\beta}$ controller based on sine-cosine algorithm (SCA) for high-order continuous interval plant (HOCIP) using a model order reduction technique. For controller design, HOCIP is initially diminished to reduced-order continuous interval plant (ROCIP) using the modified Routh–Pade approximation technique. The denominator polynomial of ROCIP is derived using modified Routh approximation which always guarantees the stability and the numerator polynomial is obtained by matching TMs and MPs that improve the transient and steady-state response of the ROCIP. Then, SCA algorithm is used to determine the five unknown parameters of $PI^{\alpha}D^{\beta}$ controller for ROCIP. The values of controller parameter are determined by minimizing two non-linear equations. For the design of $PI^{\alpha}D^{\beta}$ controller, gain crossover frequency (ω_{gc}) and phase margin (ϕ_{pm}) are considered as performance criteria. The simulation results demonstrate that the desired frequency domain specifications for both ROCIP and HOCIP are approximately fulfilled with the proposed SCA-based FOPID controller. Thus, it is established that proposed technique is an excellent alternative approach for the design of an FOPID controller using

reduced-order modeling. The future line of work for the proposed technique lies in the design of a controller for multi-input-multi-output (MIMO) continuous and discrete interval systems.

Author Contributions: The paper was a collaborative effort among the authors. Conceptualization, methodology and simulation, J.K.B, N.P., T.V.; validation and formal analysis, J.K.B.; visualization and supervision, V.P.S. All authors have read and agreed to the published version of the manuscript.

Funding: The work reported herewith has been financially supported by SERB grant (Ref.: ECR/2017/000212).

Acknowledgments: SERB grant (ECR/2017/000212).

Conflicts of Interest: The authors declare no conflict of interest.

Abbreviations

The following abbreviations are used in this manuscript:

FOPID	fractional-order proportional-integral-derivative
PM	phase margin
MPs	Markov parameters
TMs	time moments
ROCIP	reduced-order continuous interval plant
HOCIP	high-order continuous interval plant
SCA	sine-cosine algorithm
SISO	single-input-single-output
MIMO	multi-input-multi-output
PID	proportional-integral-derivative
IOPID	integer-order proportional-integral-derivative
AVR	automatic voltage regulator
MOR	model order reduction
ISE	integral-square-error
PSO	particle swarm optimization
RL	Riemann–Liouville
GL	Grunwald–Letnikov

References

1. Cruz-Zavala, E.; Moreno, J.A. Homogeneous high order sliding mode design: A Lyapunov approach. *Automatica* **2017**, *80*, 232–238. [CrossRef]
2. Almabrok, A.; Psarakis, M.; Dounis, A. Fast Tuning of the PID Controller in An HVAC System Using the Big Bang–Big Crunch Algorithm and FPGA Technology. *Algorithms* **2018**, *11*, 146. [CrossRef]
3. Yang, G.; Yi, H.; Chai, C.; Huang, B.; Zhang, Y.; Chen, Z. Predictive current control of boost three-level and T-type inverters cascaded in wind power generation systems. *Algorithms* **2018**, *11*, 92. [CrossRef]
4. Singh, S.; Singh, V.; Singh, V. Analytic hierarchy process based approximation of high-order continuous systems using TLBO algorithm. *Int. J. Dyn. Control.* **2019**, *7*, 53–60. [CrossRef]
5. Nguyen, V.G.; Guo, X.; Zhang, C.; Tran, X.K. Parameter Estimation, Robust Controller Design and Performance Analysis for an Electric Power Steering System. *Algorithms* **2019**, *12*, 57. [CrossRef]
6. Caponetto, R.; Machado, J.T.; Murgano, E.; Xibilia, M.G. Model Order Reduction: A Comparison between Integer and Non-Integer Order Systems Approaches. *Entropy* **2019**, *21*, 876. [CrossRef]
7. Singh, V.P.; Chandra, D. Model reduction of discrete interval system using dominant poles retention and direct series expansion method. In Proceedings of the 2011 5th International Power Engineering and Optimization Conference, Shah Alam, Selangor, 6–7 June 2011; pp. 27–30.
8. Zhang, S.; Yu, Y.; Wang, H. Mittag-Leffler stability of fractional-order Hopfield neural networks. *Nonlinear Anal. Hybrid Syst.* **2015**, *16*, 104–121. [CrossRef]
9. Zhang, S.; Yu, Y.; Wang, Q. Stability analysis of fractional-order Hopfield neural networks with discontinuous activation functions. *Neurocomputing* **2016**, *171*, 1075–1084. [CrossRef]
10. Monje, C.A.; Vinagre, B.M.; Feliu, V.; Chen, Y. Tuning and auto-tuning of fractional order controllers for industry applications. *Control. Eng. Pract.* **2008**, *16*, 798–812. [CrossRef]

11. Liu, L.; Tian, S.; Xue, D.; Zhang, T.; Chen, Y. Continuous fractional-order zero phase error tracking control. *ISA Trans.* **2018**, *75*, 226–235. [CrossRef]
12. Magin, R.; Ovadia, M. Modeling the cardiac tissue electrode interface using fractional calculus. *J. Vib. Control.* **2008**, *14*, 1431–1442. [CrossRef]
13. Lassoued, A.; Boubaker, O. Dynamic analysis and circuit design of a novel hyperchaotic system with fractional-order terms. *Complexity* **2017**, *2017*. [CrossRef]
14. Bingul, Z.; Karahan, O. Comparison of PID and FOPID controllers tuned by PSO and ABC algorithms for unstable and integrating systems with time delay. *Optim. Control. Appl. Methods* **2018**, *39*, 1431–1450. [CrossRef]
15. Pitolli, F. A Collocation Method for the Numerical Solution of Nonlinear Fractional Dynamical Systems. *Algorithms* **2019**, *12*, 156. [CrossRef]
16. Saleem, O.; Awan, F.G.; Mahmood-ul Hasan, K.; Ahmad, M. Self-adaptive fractional-order LQ-PID voltage controller for robust disturbance compensation in DC-DC buck converters. *Int. J. Numer. Model. Electron. Netw. Devices Fields* **2020**, *33*, e2718. [CrossRef]
17. Alamdar Ravari, M.; Yaghoobi, M. Optimum design of fractional order pid controller using chaotic firefly algorithms for a control CSTR system. *Asian J. Control.* **2019**, *21*, 2245–2255. [CrossRef]
18. Debbarma, S.; Saikia, L.C.; Sinha, N. Automatic generation control using two degree of freedom fractional order PID controller. *Int. J. Electr. Power Energy Syst.* **2014**, *58*, 120–129. [CrossRef]
19. Podlubny, I. Fractional-order systems and fractional-order controllers. *Inst. Exp. Phys. Slovak Acad. Sci. Kosice* **1994**, *12*, 1–18.
20. Aghababa, M.P. Optimal design of fractional-order PID controller for five bar linkage robot using a new particle swarm optimization algorithm. *Soft Comput.* **2016**, *20*, 4055–4067. [CrossRef]
21. Mohsenipour, R.; Fathi Jegarkandi, M. Robust stability analysis of fractional-order interval systems with multiple time delays. *Int. J. Robust Nonlinear Control.* **2019**, *29*, 1823–1839. [CrossRef]
22. Azarmi, R.; Tavakoli-Kakhki, M.; Fatehi, A.; Sedigh, A.K. Robustness analysis and design of fractional order Iλ Dμ controllers using the small gain theorem. *Int. J. Control.* **2020**, *93*, 449–461. [CrossRef]
23. Liu, L.; Zhang, S. Robust fractional-order PID controller tuning based on Bode's optimal loop shaping. *Complexity* **2018**, *2018*. [CrossRef]
24. Saidi, B.; Amairi, M.; Najar, S.; Aoun, M. Bode shaping-based design methods of a fractional order PID controller for uncertain systems. *Nonlinear Dyn.* **2015**, *80*, 1817–1838. [CrossRef]
25. Bhookya, J.; Jatoth, R.K. Optimal FOPID/PID controller parameters tuning for the AVR system based on sine–cosine-algorithm. *Evol. Intell.* **2019**, *12*, 725–733. [CrossRef]
26. Mirjalili, S. SCA: A sine cosine algorithm for solving optimization problems. *Knowl. Based Syst.* **2016**, *96*, 120–133. [CrossRef]
27. Khezri, R.; Oshnoei, A.; Tarafdar Hagh, M.; Muyeen, S. Coordination of heat pumps, electric vehicles and AGC for efficient LFC in a smart hybrid power system via SCA-based optimized FOPID controllers. *Energies* **2018**, *11*, 420. [CrossRef]
28. Kumar, M.S.; Begum, G. Model order reduction of linear time interval system using stability equation method and a soft computing technique. *Adv. Electr. Electron. Eng.* **2016**, *14*, 153–161. [CrossRef]
29. Singh, V.; Chauhan, D.P.S.; Singh, S.P.; Prakash, T. On time moments and Markov parameters of continuous interval systems. *J. Circuits Syst. Comput.* **2017**, *26*, 1750038. [CrossRef]
30. Choudhary, A.K.; Nagar, S.K. Order reduction techniques via Routh approximation: A critical survey. *IETE J. Res.* **2019**, *65*, 365–379. [CrossRef]
31. Potturu, S.R.; Prasad, R. Qualitative Analysis of Stable Reduced Order Models for Interval Systems Using Mixed Methods. *IETE J. Res.* **2018**, 1–9. [CrossRef]
32. Vijaya Anand, N.; Siva Kumar, M.; Srinivasa Rao, R. A novel reduced order modeling of interval system using soft computing optimization approach. *Proc. Inst. Mech. Eng. Part J. Syst. Control. Eng.* **2018**, *232*, 879–894. [CrossRef]
33. Potturu, S.R.; Prasad, R. Model Order Reduction of LTI Interval Systems Using Differentiation Method Based on Kharitonov's Theorem. *IETE J. Res.* **2019**, 1–17. [CrossRef]
34. Dulf, E.H. Simplified Fractional Order Controller Design Algorithm. *Mathematics* **2019**, *7*, 1166. [CrossRef]
35. Kumar Deveerasetty, K.; Nagar, S. Model order reduction of interval systems using an arithmetic operation. *Int. J. Syst. Sci.* **2020**, *51*, 886–902. [CrossRef]

36. Deveerasetty, K.K.; Zhou, Y.; Kamal, S.; Nagar, S.K. Computation of Impulse-Response Gramian for Interval Systems. *IETE J. Res.* **2019**, 1–15. [CrossRef]
37. Dewangan, P.; Singh, V.; Sinha, S. Improved Approximation for SISO and MIMO Continuous Interval Systems Ensuring Stability. *Circuits Syst. Signal Process.* **2020**, 1–12. [CrossRef]
38. Bia, P.; Mescia, L.; Caratelli, D. Fractional calculus-based modeling of electromagnetic field propagation in arbitrary biological tissue. *Math. Probl. Eng.* **2016**, *2016*. [CrossRef]
39. Shen, X. Applications of Fractional Calculus In Chemical Engineering. Ph.D. Thesis, Université d'Ottawa/University of Ottawa, Ottawa, ON, Canada, 2018.
40. ortigueira, M.D.; Tenreiro Machado, J. Fractional calculus applications in signals and systems. *Signal Process.* **2006**, *86*, 2503–2504. [CrossRef]
41. Douglas, J.F. Some applications of fractional calculus to polymer science. *Adv. Chem. Phys.* **1997**, *102*, 121–192.
42. Oldham, K.B. Fractional differential equations in electrochemistry. *Adv. Eng. Softw.* **2010**, *41*, 9–12. [CrossRef]
43. Bao, C.; Pu, Y.; Zhang, Y. Fractional-order deep backpropagation neural network. *Comput. Intell. Neurosci.* **2018**, *2018*, 7361628. [CrossRef] [PubMed]
44. Kulish, V.V.; Lage, J.L. Application of fractional calculus to fluid mechanics. *J. Fluids Eng.* **2002**, *124*, 803–806. [CrossRef]
45. Magin, R.L. *Fractional Calculus in Bioengineering*; Begell House: Redding, CA, USA, 2006; Volume 2.
46. Soriano-Sánchez, A.G.; Rodríguez-Licea, M.A.; Pérez-Pinal, F.J.; Vázquez-López, J.A. Fractional-order approximation and synthesis of a PID controller for a buck converter. *Energies* **2020**, *13*, 629. [CrossRef]
47. Petráš, I. *Fractional-Order Nonlinear Systems: Modeling, Analysis and Simulation*; Springer Science & Business Media: Berlin/Heidelberg, Germany, 2011.
48. Gu, D.W.; Petkov, P.; Konstantinov, M.M. *Robust control design with MATLAB®*; Springer Science & Business Media: Berlin/Heidelberg, Germany, 2005.
49. Tarasov, V.E.; Tarasova, S.S. Fractional derivatives and integrals: What are they needed for? *Mathematics* **2020**, *8*, 164. [CrossRef]
50. Tejado, I.; Vinagre, B.M.; Traver, J.E.; Prieto-Arranz, J.; Nuevo-Gallardo, C. Back to basics: Meaning of the parameters of fractional order PID controllers. *Mathematics* **2019**, *7*, 530. [CrossRef]
51. Khubalkar, S.; Chopade, A.; Junghare, A.; Aware, M.; Das, S. Design and realization of stand-alone digital fractional order PID controller for Buck converter fed DC motor. *Circuits Syst. Signal Process.* **2016**, *35*, 2189–2211. [CrossRef]
52. Sondhi, S.; Hote, Y.V. Fractional order controller and its applications: A review. *Proc. AsiaMIC* **2012**. [CrossRef]
53. Podlubny, I. Fractional-order systems and PI/sup/spl lambda//D/sup/spl mu//-controllers. *IEEE Trans. Autom. Control.* **1999**, *44*, 208–214. [CrossRef]
54. Nise, N.S. *Control Systems Engineering*; John Wiley & Sons: Hoboken, NJ, USA, 2020.
55. Ortigueira, M.D.; Trujillo, J.J.; Martynyuk, V.I.; Coito, F.J. A generalized power series and its application in the inversion of transfer functions. *Signal Process.* **2015**, *107*, 238–245. [CrossRef]
56. Dolgin, Y. Author's reply [to comments on'On Routh-Pade model reduction of interval systems']. *IEEE Trans. Autom. Control.* **2005**, *50*, 274–275. [CrossRef]
57. Vinagre, B.M.; Monje, C.A.; Calderón, A.J.; Suárez, J.I. Fractional PID controllers for industry application. A brief introduction. *J. Vib. Control.* **2007**, *13*, 1419–1429. [CrossRef]
58. Monje, C.A.; Calderon, A.J.; Vinagre, B.M.; Chen, Y.; Feliu, V. On fractional PI λ controllers: Some tuning rules for robustness to plant uncertainties. *Nonlinear Dyn.* **2004**, *38*, 369–381. [CrossRef]
59. Yeroglu, C.; Tan, N. Note on fractional-order proportional–integral–differential controller design. *IET Control. Theory Appl.* **2011**, *5*, 1978–1989. [CrossRef]
60. Pal, J. System reduction by a mixed method. *IEEE Trans. Autom. Control.* **1980**, *25*, 973–976. [CrossRef]
61. Singh, V. Sine cosine algorithm based reduction of higher order continuous systems. In Proceedings of the 2017 International Conference on Intelligent Sustainable Systems (ICISS), Palladam, India, 7–8 December 2017; pp. 649–653.
62. Srivastava, S.; Singh, V.; Singh, S.; Dohare, R.; Kumar, S. Luus-Jaakola based PID controller tuning for double tank system. *Int. J. Adv. Technol. Eng. Explor.* **2016**, *3*, 199. [CrossRef]
63. Singh, V.P.; Chandra, D.; Rastogi, R. Luus jaakola algorithm based order reduction of discrete interval systems. *Pratibha Int. J. Sci. Spirit. Bus. Technol. IJSSBT* **2012**, *1*, 1–8.

64. Prakash, T.; Singh, S.; Singh, V. Analytic hierarchy process-based model reduction of higher order continuous systems using sine cosine algorithm. *Int. J. Syst. Control. Commun.* **2020**, *11*, 52–67. [CrossRef]
65. Mehra, S.; Monga, H.; Singh, V.; Kumar, R. Application of SCA for Level Control of Three-Tank System. In Proceedings of the 2020 International Conference on Computation, Automation and Knowledge Management (ICCAKM), Dubai, UAE, 9–10 January 2020; pp. 220–224.
66. Thakur, A.; Monga, H.; Singh, V.; Kumar, R.; Mathur, A. Sine Cosine Algorithm Assisted Tuning of PID Controller for DC Servo-Motor. In Proceedings of the 2020 International Conference on Computation, Automation and Knowledge Management (ICCAKM), Dubai, UAE, 9–10 January 2020; pp. 230–233.